

# Fate Modelling of DEHP in Roskilde Fjord, Denmark

Patrik Fauser · Jørgen Vikelsøe · Peter B. Sørensen ·  
Lars Carlsen

Received: 31 October 2006 / Accepted: 31 July 2008 / Published online: 16 August 2008  
© Springer Science + Business Media B.V. 2008

**Abstract** The fate of di(2-ethylhexyl)phthalate (DEHP) is modeled in Roskilde fjord, Denmark. The fjord is situated near Roskilde, which comprises 80,000 PE, various industries, a central wastewater treatment plant, and adjacent agricultural fields. Roskilde fjord is thus a suitable recipient for studying the transport and fate of DEHP, which is used in a variety of different industries and consumer products. Wastewater from households and industries is led to the local wastewater treatment plant, which leads the effluent to the fjord. The sludge is partly stored and partly amended on an adjacent field. The model applied in the present study is a simple box model coupling water and sediment compartments of the fjord with wastewater treatment plant effluent, streams leading to the fjord, and atmospheric deposition. The fjord model comprises first-order degradation, adsorption, sedimentation,

vertical diffusion in the sediment, dispersive mixing in the water, and water exchange with the surrounding sea. Experimental measurements of DEHP were made in the fjord water and sediment, in the wastewater treatment plant inlet and effluent, and in streams and atmospheric deposition. The experimental data are used to calibrate the model. The model results show that freshwater from streams is the predominant DEHP source to the fjord, followed by atmospheric deposition and effluents from wastewater treatment plants. Sedimentation is the predominant removal mechanism followed by water exchange with the sea and degradation.

**Keywords** Fate model · Phthalates · DEHP · Fjord · Sediment

## 1 Introduction

Chemicals enter the environment via many sources, and once they are emitted their transport patterns can be complex. In some cases, the origin and fate of a chemical may be clear and easy to track in the environment, such as the washing detergent linear alkylbenzene sulfonate, which is predominantly emitted to the wastewater. In other cases, the chemical may be present in a wide range of products and used in many different industrial and household activities. Thus, the phthalate ester di(2-ethylhexyl)phthalate (DEHP) is the most abundantly used phthalate ester and is primarily used in polyvinyl chloride (PVC) products as softener. The content of DEHP in flexible polymer materials varies but is often around 30% (w/w) [9]. Flexible PVC is used in many different articles, e.g., toys, building material such as flooring, cables, profiles, and roofs, as well as medical products like blood bags, dialysis equipment,

---

P. Fauser (✉)  
Department of Policy Analysis,  
National Environmental Research Institute,  
Frederiksborgvej 399, Post Box 358, 4000 Roskilde, Denmark  
e-mail: paf@dmu.dk

J. Vikelsøe  
Department of Atmospheric Environment,  
National Environmental Research Institute,  
Frederiksborgvej 399, Post Box 358, 4000 Roskilde, Denmark

P. B. Sørensen  
Department of Terrestrial Ecology,  
National Environmental Research Institute,  
Vejløvej 25, Post Box 314, 8600 Silkeborg, Denmark

L. Carlsen  
Awareness Center,  
Hyldeholm 4, Veddelev,  
4000 Roskilde, Denmark

etc. DEHP is used also in other polymer products and in other nonpolymer formulations and products [1, 17]. Consequently, the wide use of DEHP gives rise to many possible scenarios of human and environmental exposure. Considering the suspected hormone-disrupting effects (risk phrases R60 and R61) and the large annual use of 73,500-ton PVC in Denmark alone [16], a risk assessment has been undertaken for DEHP [1]. The conclusions for the environment are that there is at present no need for further information and/or testing for wastewater treatment plants, surface water, sediment, the atmospheric compartment, and the terrestrial compartment. For human health, there is need for limiting the risks for human health for workers, consumers (children, patients), man exposed indirectly via the environment (adults, children, babies or infants), and combined exposure [1].

In order to implement the restrictive regulations suggested in a risk assessment, a coupling between source and target is required. This is inherent in a fate, or cycle, analysis of the chemical in the environment. Although DEHP is predominantly used in PVC products, it is not evident that the fate of DEHP follows the fate of the PVC products. The objective of this study is to follow the cycle of DEHP in a typical Danish rural environment and to define the main sources and removal mechanisms with respect to the recipient Roskilde fjord.

Fjords and inner waters have been investigated with a variety of models ranging from simple batch reactor models describing residence time (e.g., [5]) to more complex models such as MARE (MARine Research on Eutrophication) that builds on a series of models linking information about ecosystem properties, biogeochemical processes, physical transport, nutrient inputs, and costs for nutrient reductions [15]. Further studies on fate modeling of phthalate esters in environmental matrices can be found in Kao et al. [8], Turner and Rawling [19], Williams et al. [23], and Zhou and Liu [24].

In the present work, we use a model that includes all significant spatial and temporal trends of the DEHP flow in Roskilde fjord, and yet so simple that the number of input parameter is minimal. In this way, the uncertainty related to parameter uncertainty will be minimized and the predictive power of the analysis will be optimized. The model is evaluated theoretically and with experimental measurements.

## 2 Background and Theory

Roskilde fjord cuts its way through northern Zealand. It is approximately 40 km long and ends in the northern part of the Isefjord (Fig. 1). The total surface area is approximately 125 km<sup>2</sup>; mean depth is 3 m and maximum depth is 31 m at

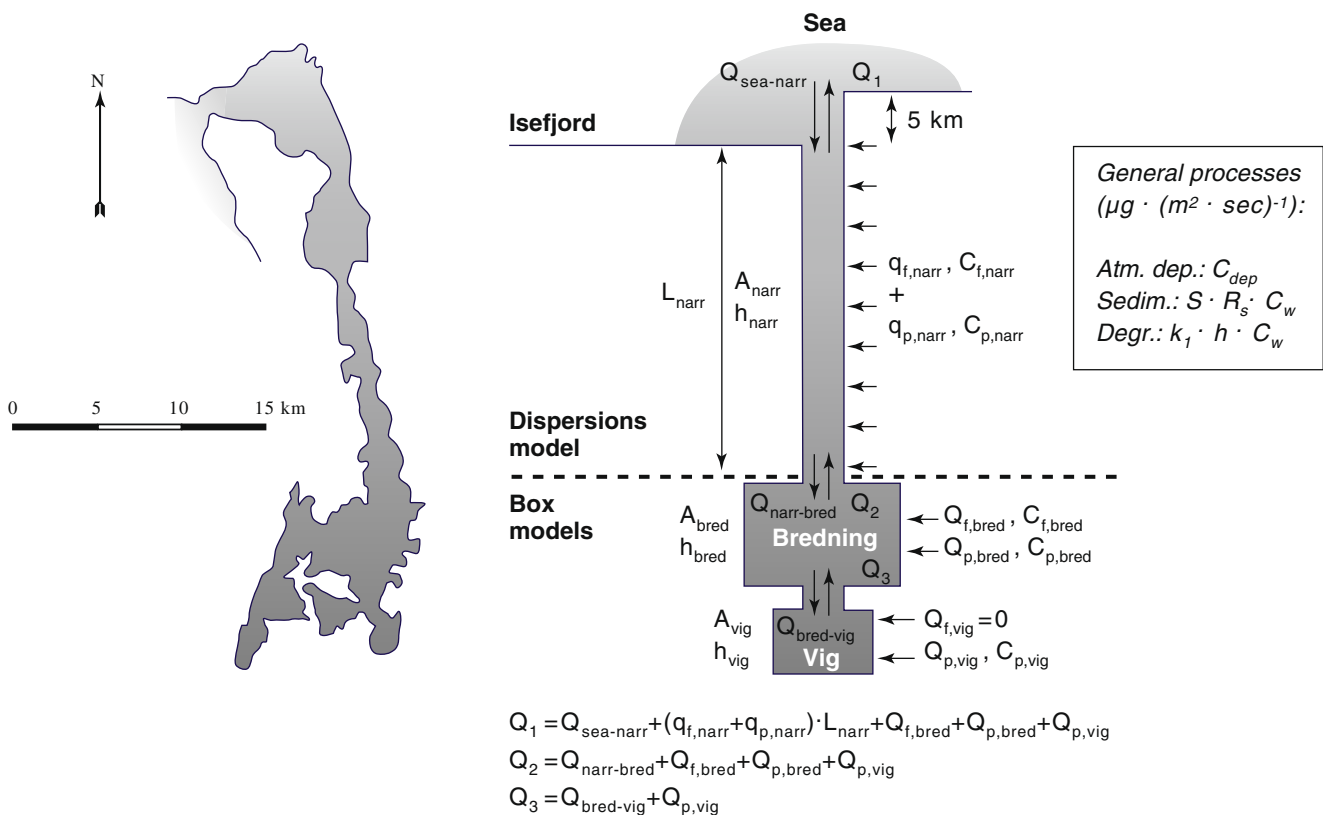


**Fig. 1** Schematic view of Roskilde fjord. Symbols and notations are explained in Table 1

the end of Lejre Vig. A shallow threshold that causes a long residence time in the southern part separates the northern and southern parts. Surveillance of Roskilde fjord is performed annually in the Danish national monitoring program NOVANA (e.g., [22]) where chemicals and biota are monitored in the aquatic and terrestrial environment.

The level and the temporal and spatial variation of DEHP concentrations were measured in Roskilde fjord during three seasonal campaigns, involving widespread different locations. Sediments were investigated in the innermost part of the fjord (Roskilde Vig) including a core 22 cm deep (~80 years old) [20]. The seasonal sampling additionally comprised atmospheric deposition, three streams, and a lake, including water and sediment. Furthermore, DEHP concentrations were measured in the particulate and dissolved phases at the inlet, effluent, and sludge at the wastewater treatment plant (WWTP). Measurements and modeling of the WWTP performance is presented in Fauser et al. [2, 3]. Effluent concentrations and flows are applied as input to the fjord.

Physicochemical processes and parameters that involve the fate of DEHP in the water and sediment, respectively, are:

- *Bio-degradation*; Different first-order degradation rates,  $k_1$  values, can be found in the literature for the degradation of DEHP in water and sediment, respectively. In the water phase, the concentration of active biomass is very small and as a rough estimate a reaction rate equal to a factor of 1,000 [4] lower than the aerobic rate found in a WWTP  $k_1=10^{-5} \text{ s}^{-1}$  by Fauser et al. [3] is expected. Slow degradation has also been found in the terrestrial environment, probably due to anaerobic conditions [21]. In the aerobic sediment, surface layer about the same degradation rate as in the WWTP is expected. The thickness of the layer can be varying, mainly due to wind conditions and a probable mean value will be around 5 cm. Below this layer, anoxic (nitrate or sulfate-reducing) conditions prevail and a degradation rate factor of 10 lower than the aerobic rate is assumed.
- *Sorption*; At the WWTP outlet and in the water phase of the fjord, the organic fraction of the particulate matter is relatively high and in the sediment it is lower due to degradation, implying a lower  $K_d$  value in the sediment. However,  $K_d$  is defined under equilibrium conditions and since it is questionable whether the retention time in the water is long enough for equilibrium to occur, a reduction of the sorption coefficient is appropriate in the water. On the other hand, the substance entering the fjord through discharge and deposition will already be associated to DOM and therefore it is more a problem of desorption

in the diluted fjord water. At the sediment surface, the organic fraction will be higher than in the deeper layers. The sediment density is, however, assumed to be constant throughout the depth although there will be an increase caused by pressure buildup. The former will result in a decreasing sorption coefficient and the latter in an increasing sorption coefficient for increasing depths. Microbial degradation of organic matter can release adsorbed substance. Digestion of organic matter by benthic organisms will remove adsorbed substance and degrade or incorporate it in the tissue. The substance will then be released as adsorbed substance when the organism dies. The former process will result in a decreasing sorption coefficient and the latter process an increasing sorption coefficient. Due to these complex interactions, only one  $K_d$  value is assigned to the total system. In the WWTP, a  $K_d$  value for DEHP was found to be approximately  $13,000 \text{ L kgDM}^{-1}$  [2]. The organic content in the sediment and in the particulate material in the WWTP effluent and fjord water is lower than in the biomass in the bioreactors in the WWTP, and a  $K_d$  value of 10,000 is applied.

- *Sedimentation* is a transport mechanism where particles are brought to the sediment surface by gravitational settling. Due to turbulence resuspension of surface layer, particles will occur. The resuspended particles are assumed to comprise the same concentration of adsorbed substance as the particles in the water phase. It is therefore sufficient to consider the net sedimentation. DEHP occurs in low concentrations and has low solubility and low degradation rate [18]. The governing removal or transport mechanism in the sediment is diffusion, which in turn is related to a similar removal rate from the water phase. The approach is therefore to define the vertical transport of nonsedimentary substance in terms of a “suction” caused by molecular concentration gradient conditioned diffusion in the sediment, where the water depth is 3 m and the dry matter content at the surface is  $1.58 \text{ kg org. dm L}^{-1}$ . Madsen and Larsen [10] found linear accumulation rates in the inner fjord in the interval  $1.2\text{--}5.8 \text{ mm year}^{-1}$ . The total downward transport of substance is thus found from a combination of diffusive concentration gradient conditioned transport and sedimentation of adsorbed particulate substance.
- *Vertical transport in the sediment*; Once the substances have reached the sediment, the dissolved fraction can be transported further vertically and horizontally. The flux in the sediment is governed by molecular diffusion. Advection and convection are negligible processes that are primarily relevant in connection with hydraulic gradients in groundwater studies. The relationship between molecular size and diffusivity can be

used to predict diffusivities of compounds from known diffusivities of other compounds based alone on the molecular masses, cf. Eq. 1 [12].

$$\frac{D_{\text{unknown}}}{D_{\text{known}}} \approx \sqrt{\frac{M_{\text{w,known}}}{M_{\text{w,unknown}}}} \quad (1)$$

This requires that the carrier media are the same and that the chemical structures are related. Benzene may be used as a model compound for calculating the diffusivity of DEHP that also contain a benzene ring in addition to the alkyl chains and ester groups. Schwarzenbach et al. [12] have found  $D_{\text{benzene}}=10^{-9} \text{ m}^2 \text{ s}^{-1}$  ( $M_{\text{w,benzene}}=78 \text{ g mol}^{-1}$ ). Combined with  $M_{\text{w,DEHP}}=391 \text{ g mol}^{-1}$ , this yields  $D_{\text{DEHP}}=5 \times 10^{-10} \text{ m}^2 \text{ s}^{-1}$ . Fick's first law can describe the vertical substance flux in the sediment

$$N_{\text{sz}}=\theta \times D_{\text{disp,sz}} \times \frac{dC_{\text{s}}}{dz} \left[ \frac{\text{mg}}{\text{m}^2\text{s}} \right] \quad (2)$$

where  $\theta=0.55$ -L water (per liter total) is the porosity of the sediment and  $D_{\text{disp,sz}}$  is the vertical dispersion coefficient in the sediment and  $C_{\text{s}}$  the sediment DEHP concentration. Schwarzenbach et al. [12] suggest the following empirical relationship to the molecular diffusivity

$$\begin{aligned} D_{\text{disp,sz}} &= D_{\text{DEHP}} \times \theta^{1.5} = 5 \times 10^{-10} \times 0.55^{1.5} \\ &= 2 \times 10^{-10} \frac{\text{m}^2}{\text{s}} \end{aligned} \quad (3)$$

Neglecting the influence from bioturbation, the horizontal concentration gradient is much smaller than the vertical concentration gradient and the horizontal diffusion can be omitted in the mass balance for a model sediment volume.

- *Horizontal transport in the water*; The hydraulic effect from the sea will cause a high flow through the narrow parts in the middle of the fjord. This combination of saline intrusions and freshwater discharges causes a salinity gradient ranging from 20‰ in the northern entrance to 14.5‰ in the inner parts of the fjord [6]. On a local scale, freshwater intrusions can enter the saline fjord and thus lower the salinity. However, it is assumed that the convective flow in the sediment is

zero, thus excluding the influence of percolation of groundwater through the sediment into the fjord. Only net deposition, streams, and anthropogenic outlets are considered as freshwater sources to the fjord. Due to an effective large-scale mixing of the water volumes, which enhances the vertical transport of dissolved and particulate matter, the vertical concentration gradient is negligible, resulting in a mean depth-integrated concentration in the water column. The large-scale mixing, which is caused by a combination of wind- and current-driven turbulence and convection, is also the predominant process in the horizontal transport of water and substances. Tides are shallow within the inner Danish waters and have only limited influence on potential mixing and water exchange due to tidal gates in the estuaries and fjords to the North Sea. Hydraulic effects from wind and freshwater sources are able to create water-level fluctuations up to 170 cm above mean sea level in the inner fjord compared to only  $\pm 10$  cm resulting from tidal variations [11]. The salinity mixing data are used to calculate an effective longitudinal dispersion coefficient for the narrow part of the fjord. Assuming a uniformly distributed freshwater supply along the shore of  $1.16 \times 10^{-4} \text{ m}^3 (\text{m s})^{-1}$ , a mean cross-sectional area of  $2,610 \text{ m}^2$ , a length of 28 km, cf. Table 1, and salinities of 20‰ in the northern entrance and 14.5‰ in the Bredning, the effective dispersion coefficient can be calculated from the salinity gradient [6]

$$D_{\text{wx}} = \frac{1.16 \times 10^{-4} \frac{\text{m}^3}{\text{s}} \times (28,000\text{m})^2}{2 \times 2610\text{m}^2 \times \ln \frac{20.0}{14.5}} = 54 \frac{\text{m}^2}{\text{s}} \quad (4)$$

The longitudinal salinity gradient is only constant in the narrow part of the fjord and therefore the dispersion coefficient is only representative of this section. In the inner fjord where the discharge from the WWTP is situated, the salinity is approximately constant and the horizontal transport is based on wind-driven turbulence and convective mixing. Conclusively, it is not relevant to consider the transport in the Vig and Bredning in relation to dispersion but rather to consider them as mixed basins.

**Table 1** Hydraulic and geographical key data for Roskilde Vig, Bredning, and narrow passage

	Vig	Bredning	Narrow passage
Surface area	$A_{\text{vig}}=4 \text{ km}^2$	$A_{\text{bred}}=48 \text{ km}^2$	$A_{\text{narr}}=73 \text{ km}^2$
Length	–	$L_{\text{bred}}=(10 \text{ km})$	$L_{\text{narr}}=28 \text{ km}$
Mean depth	$h=3 \text{ m}$	$h=3 \text{ m}$	$h=3 \text{ m}$
Diffuse freshwater flow	$Q_{\text{f,vig}}=0$	$Q_{\text{f,bred}}=3.60 \text{ m}^3 \text{ s}^{-1}$	$q_{\text{f,narr}}=1.16 \times 10^{-4} \text{ m}^3 (\text{m s})^{-1}$
Point source flow	$Q_{\text{p,vig}}=136.7 \times 10^{-3} \text{ m}^3 \text{ s}^{-1}$	$Q_{\text{p,bred}}=36.0 \times 10^{-3} \text{ m}^3 \text{ s}^{-1}$	$q_{\text{p,narr}}=3.60 \times 10^{-6} \text{ m}^3 (\text{m s})^{-1}$
Water exchange	$Q_{\text{bred-vig}}=(0.5 \times Q_{\text{f,sea}}) 3.4 \text{ m}^3 \text{ s}^{-1}$	$Q_{\text{narr-bred}}=(2 \times Q_{\text{f,sea}}) 13.7 \text{ m}^3 \text{ s}^{-1}$	$Q_{\text{sea-narr}}=(3 \times Q_{\text{f,sea}}) 20.5 \text{ m}^3 \text{ s}^{-1}$

### 3 Sources

WWTP effluent is discharged as a point source to the surface water at the shore at the innermost part of Roskilde fjord (Vig). The flow is  $492 \pm 356 \text{ m}^3 \text{ day}^{-1}$  with a mean concentration of  $0.7 \text{ } \mu\text{g DEHP per cubic meter}$  [2, 3]. Point sources to the Bredning and narrow passage of the fjord, i.e., WWTP discharges from four smaller cities, are estimated to account for the same concentration ( $C_{\text{WWTP}}$ ) and flow rate ( $Q_{\text{WWTP}}$ ) as the WWTP in the Vig. The total load from the point sources is distributed uniformly along the horizontal axis (cf. Table 1 and Fig. 1). Freshwater intrusions from streams and lakes occur along Roskilde Bredning and the narrow passage. The freshwater intrusion is higher per length unit in the Bredning than in the narrow passage. Atmospheric deposition is considered to be uniformly distributed with respect to time and surface area. The dry deposition rate is  $230 \text{ } \mu\text{g DEHP (m}^2 \text{ year)}^{-1}$  [21]. For a period of 25 years, ending in 1991, all sludge produced in earlier WWTPs in Roskilde was used for amendment on an agricultural field adjacent to the WWTP discharge. Since 1991, the produced sludge has been stored in an intermediary deposit close to the sludge-amended area and shore. Leaching from the sludge-amended soil as well as washout from the sludge deposit, in case of heavy rainfall, contribute to the load to the fjord [21]. In 1969, in connection with work on the Roskilde harbor, the sediment was dumped nearby in the fjord. This has since then been a source of leaching to the fjord water. The load has decreased with time and is today estimated to be negligible compared to the WWTP discharge. The flux of saline water from the sea to the fjord is three to four times larger than the freshwater flux to the fjord [7]. In Table 1, water exchange rates are stated.

### 4 Model Parameters

Parameters are either required as input or are estimated from model runs. They are state variables, i.e., dependent variables that are being modeled, model inputs, i.e., constants required to run the model, calibration parameters, i.e., constants used for performing an adjustment or tuning between model results and measurements.

Calculated and measured state variables:

- $C_w$  Concentration of dissolved DEHP in water phase [ $\text{mg L}^{-1}$ ].  
 $C_s$  Concentration of dissolved DEHP in sediment phase [ $\text{ng g}^{-1}$ ].

Measured model inputs:

- $X_w$  Concentration of suspended particulate matter in water phase =  $10 \times 10^{-6} \text{ kg DM (L total)}^{-1}$

- $X_s$  Concentration of dry matter in sediment =  $1.06 \text{ kg DM (L total)}^{-1}$   
 $\theta_s$  Water fraction in sediment =  $0.55 \text{ L water (L total)}^{-1}$   
 $Q_{\text{WWTP}}$  Discharge flow from WWTP =  $492 \pm 356 \text{ m}^3 \text{ h}^{-1}$   
 $C_{\text{WWTP}}$  Concentration of dissolved DEHP in WWTP discharge =  $0.7 \text{ } \mu\text{g DEHP L}^{-1}$   
 $R_{\text{WWTP}}$  Retention factor for WWTP discharge = 1.05  
 $C_{\text{tot,dep}}$  Atmospheric bulk deposition =  $7.29 \times 10^{-15} \text{ kg DEHP (m}^2 \text{ s)}^{-1}$   
 $C_{\text{tot,f}}$  Concentration of mean total substance in freshwater from streams =  $0.2 \text{ } \mu\text{g DEHP L}^{-1}$

Calibration parameters:

- $K_d$  Distribution coefficient between water and organic matter in water or sediment [ $\text{L water (kg DM)}^{-1}$ ].  
 $k_{\text{IN}}$  Aerobic pseudo first-order removal rate [ $\text{s}^{-1}$ ].  
 $k_{\text{ID}}$  Anaerobic pseudo first-order removal rate [ $\text{s}^{-1}$ ].  
 $S$  Annual sediment accumulation rate [ $\text{mm year}^{-1}$ ].

Estimated model inputs:

- $D_{\text{wx}}$  Horizontal dispersion coefficient in narrow part of fjord =  $54 \text{ m}^2 \text{ s}^{-1}$   
 $D_{\text{sz}}$  Molecular diffusion coefficient in sediment =  $2 \times 10^{-10} \text{ m}^2 \text{ s}^{-1}$

and parameters in Table 1.

The mean residence time for the entire fjord is approximately 3 months.

### 5 Model Equations

Roskilde Vig and Bredning are considered to be totally mixed and the narrow part of the fjord is described by dispersion. A water model and a sediment model is set up that in combination describe the dynamic and steady-state DEHP concentrations in the water and sediment of Roskilde fjord and account for the overall mass balances in the different regions of the fjord. The water model is a steady-state box models of Roskilde Vig and Bredning combined with a dynamic numerical model of the narrow passage of the fjord. The sediment model is a numerical model including diffusion, sedimentation, and degradation and analytical expressions. Experimental results are used to validate the models.

The models are set up based on the assumptions of constant discharge flow ( $Q_{\text{WWTP}}$ ), freshwater flow ( $Q_f$ ), deposition ( $Q_{\text{dep}}$ ), discharge concentration ( $C_{\text{WWTP}}$ ), freshwater concentration ( $C_f$ ), deposition concentration ( $C_{\text{dep}}$ ), water depth ( $h$ ), concentrations of suspended matter in water and sediment ( $X_w$ ,  $X_s$ ), equilibrium between dissolved and adsorbed substance ( $K_d$ ). The water volume is totally mixed

along the vertical axis; there is only vertical diffusive flow in sediment ( $D_{sz}$ ); the dissolved concentration in sediment surface layer is equal to the dissolved water concentration; there is first-order degradation of dissolved substance in water and sediment ( $k_1$ ), and sediment depth is increasing in time due to sedimentation ( $S$ ).

In order to establish simple and robust models, the growth and wilting cycle of vegetation and influence of changing emission patterns from consumers and wastewater treatment plants are not considered. Accordingly, mean annual conditions are simulated based on constant flows and concentrations.

### 5.1 Steady-State Box Model for Water Compartment

The general steady-state mass balance is shown in Eq. 5 and for Roskilde Vig the mass balance becomes as shown in Eq. 6. Mass balances for Roskilde Bredning and narrow passage are described analogously. In Roskilde Vig, mass balance  $C_{w,bred}$  is unknown. In Roskilde Bredning, mass balance  $C_{w,vig}$  and  $C_{w,narr}$ (boundary) are unknown and in the mass balance for the narrow passage  $C_{w,bred}$  is unknown. By inserting model parameters and values from Table 1 and performing model iterations, the unknowns are determined.

$$0 = \text{Point sources} + \text{Freshwater sources} + \text{Water exchange} + \text{Atmospheric deposition} + \text{Sedimentation} + \text{Degradation} \Rightarrow \quad (5)$$

$$0 = C_{WWTP} \times R_{WWTP} \times Q_{WWTP} + C_{tot,f} \times Q_{f,vig} - C_{w,vig} \times R_w \times (Q_{bred-vig} + Q_{p,vig} + Q_{f,vig}) + C_{tot,dep} \times A_{vig} - C_{w,vig} \times S \times A_{vig} \times R_s - k_1 \times C_{w,vig} \times A_{vig} \times h_{vig} \quad (6)$$

### 5.2 Differential and Numerical Water and Sediment Models for Narrow Passage

The mass balance for the water compartment of the Vig and Bredning are as shown in Eq. 6. For the narrow passage, the water mass balance is described below. Transport in the sediment is described irrespective of the model for the water. In Fig. 2, a vertical section of the water–sediment system is shown and horizontal and vertical mass fluxes are stated for each compartment.

The time incremental mass balance for a water volume  $dx \times b \times h$  and a sediment volume  $dx \times b \times dz$  is shown in Eq. 7, where  $N_x$  and  $N_z$  are the mass fluxes [ $g (m^2 s)^{-1}$ ] along the  $x$ - and  $z$ -axis, respectively, of substance A with

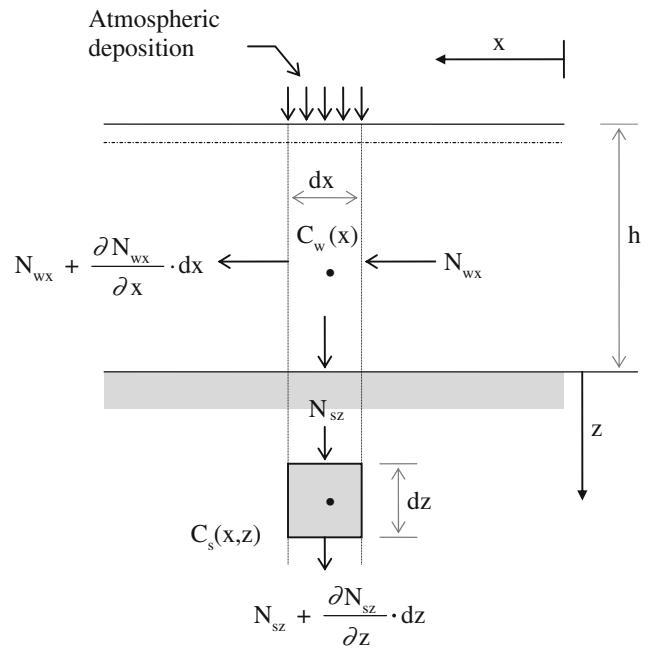


**Fig. 2** Vertical sectional view of the water–sediment system in the narrow passage of Roskilde fjord

dissolved concentration  $C_A$ .  $k_1$  is a pseudo first-order process constant. Equation 8 is the result of two-dimensional modeling assumptions and can be formulated for the water and sediment compartment, respectively.

$$\frac{dC_A}{dt} \times R \times dx \times b \times dz = N_x \times b \times dz - \left( N_x + \frac{dN_x}{dx} \times dx \right) \times b \times dz + N_z \times dx \times b - \left( N_z + \frac{dN_z}{dz} \times dz \right) \times dx \times b + \sum k_{1i} \times C_A \times dx \times b \times dz \Rightarrow \quad (7)$$

$$\frac{dC_A}{dt} = - \frac{dN_x}{dx} \times \frac{1}{R} - \frac{dN_z}{dz} \times \frac{1}{R} - \sum \frac{k_1}{R} \times C_A \quad (8)$$

#### 5.2.1 Differential Equation Water Compartment (Narrow Passage)

The horizontal flux, in Eq. 9, includes advection and dispersion

$$N_{wx} = \frac{Q_{narr}}{b \times h} \times C_{w,narr} \times R_w - D_{wx} \times \frac{\partial C_{w,narr}}{\partial x} \times R_w \quad (9)$$

where (cf. Fig. 1)

$$Q_{narr} = Q_{f,bred} + Q_{p,vig} + (q_{f,narr} + q_{p,narr}) \times x \quad (10)$$

The vertical flux, in Eq. 11, is a combination of sedimentation of particles, extraction of molecular substance through sediment suction, atmospheric deposition, and freshwater sources. The first term is the boundary condition at the sediment surface caused by sediment “suction” of substance. The total mass balance for the water compartment furthermore includes first-order degradation and thus becomes as shown in Eq. 12

$$N_{wz} = -D_{sz} \times \frac{\partial C_s}{\partial z} \Big|_{z=0} - S \times R_s \times C_{w,narr} + C_{tot,dep} + \frac{q_{f,narr}}{b} \times C_{tot,f} + \frac{q_{p,narr}}{b} \times C_{tot,p} \tag{11}$$

$$\begin{aligned} \frac{\partial C_{w,narr}}{\partial t} &= \frac{Q_{narr}}{b \times h} \times \frac{\partial C_{w,narr}}{\partial x} + \frac{(q_{f,narr} + q_{p,narr})}{b \times h} \times C_{w,narr} + \\ &D_{wx} \times \frac{\partial^2 C_{w,narr}}{\partial x^2} - \frac{D_{sz}}{R_w \times h} \times \frac{\partial C_s}{\partial z} \Big|_{z=0} + \\ &\frac{C_{dep}}{R_w \times h} - \frac{S \times R_s \times C_{w,narr}}{R_w \times h} - \frac{k_1}{R_w} \times C_{w,narr} + \\ &\frac{q_{f,narr}}{b \times h \times R_w} \times C_{tot,f} + \frac{q_{p,narr}}{b \times h \times R_w} \times C_{tot,p} \end{aligned} \tag{12}$$

Boundary conditions:

$$\begin{aligned} C_{w,narr} &= C_{w,bred} && \text{for } x = 0 \\ C_{w,narr} &= C_{w,sea} = 0 && \text{for } x = L_{narr} + 5\text{km} \end{aligned}$$

### 5.2.2 Differential Equation Sediment Compartment (Narrow Passage, Bredning, and Vig)

The horizontal flux is negligible. The vertical flux arising from molecular diffusion and advection from sediment buildup is shown in Eq. 13. The total mass balance for the sediment compartment is shown in Eq. 14. In the upper 5 cm, the aerobic degradation rate,  $k_{1N}$ , is used and further down the anoxic degradation rate,  $k_{1D}$ , is used.

$$N_{sz} = -D_{sz} \times \frac{\partial C_s}{\partial z} + S \times R_s \times C_w \tag{13}$$

$$\frac{\partial C_s}{\partial t} = \frac{D_{sz}}{R_s} \times \frac{\partial^2 C_s}{\partial z^2} - S \times \frac{\partial C_s}{\partial z} - \frac{k_1}{R_s} \times C_s \tag{14}$$

### 5.2.3 Numerical Equation Water Compartment (Narrow Passage)

The two coupled second-order differential Eqs. 12 and 14, each having two independent variables,  $x$  and  $t$  for the water model and  $z$  and  $t$  for the sediment model, respectively, can be solved numerically using a grid

consisting of discrete nodes for the  $(x, t)$  and the  $(z, t)$  system, respectively, and by employing a forward time central space scheme (cf. Fig. 3).

$$\begin{aligned} C_w^{n+1}(i) &= C_w^n(i) \\ &+ dt \times \left( \frac{Q_{narr}}{b \times h} \times \frac{(C_w^n(i+1) - C_w^n(i))}{dx} + \frac{(q_{f,narr} + q_{p,narr})}{b \times h} \times C_w^n(i) \right) \\ &+ dt \times \left( D_{wx} \times \frac{(C_w^n(i+1) - 2 \times C_w^n(i) + C_w^n(i-1)))}{dx^2} \right) \\ &- dt \times \left( \frac{D_{sz}}{R_w \times h} \times \frac{(C_s^n(i,j+1) - C_s^n(i,j))}{dz} \right) \Big|_{j=0} \\ &+ dt \times \left( \frac{C_{dep}}{R_w \times h} - \frac{S \times R_s}{R_w \times h} \times C_w^n(i) - \frac{k_1}{R_w} \times C_w^n(i) \right) \\ &+ dt \times \left( \frac{q_{f,narr}}{b \times h \times R_w} \times C_{tot,f} + \frac{q_{p,narr}}{b \times h \times R_w} \times C_{tot,p} \right) \end{aligned} \tag{15}$$

### 5.2.4 Numerical Equation Sediment Compartment (Narrow Passage, Bredning, and Vig)

The numerical interpretation of the sedimentation term  $S \times R_s \times C_w$  is accounted for by increasing the sediment thickness with an extra layer,  $dz$ , each time Eq. 16 is fulfilled. With a step size of  $dz=0.01$  m and an accumulation rate of  $S=2.5$  mm year<sup>-1</sup>, an additional layer with thickness  $dz$  must be added every 4 years. In doing so, the entire concentration profile is moved downward one grid point. The numerical difference Eq. 17 does therefore not

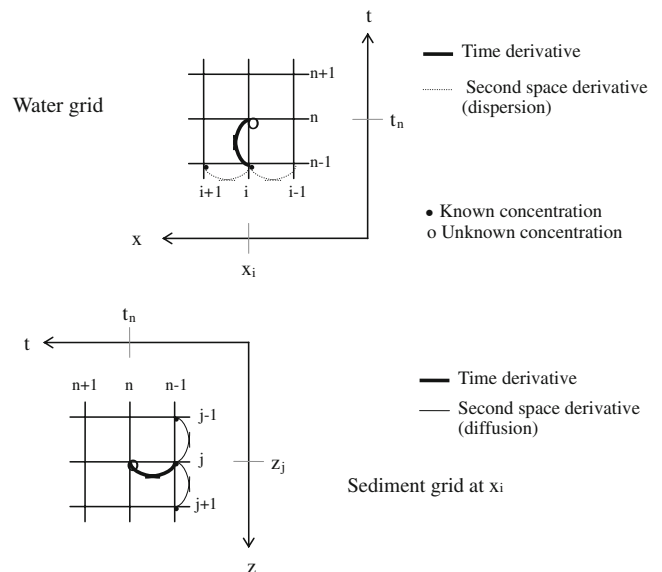


Fig. 3 Time-space grids for the water and sediment models, respectively

comprise a sedimentation term. For  $j=0$ , the second space derivative in Eq. 17 is shown in Eq. 18.

$$t_{\text{sed}} = \frac{dz}{S} \tag{16}$$

$$C_s^{n+1}(i,j) = C_s^n(i,j) + dt \times \left( \frac{D_{sz}}{R_s} \times \frac{(C_s^n(i,j+1) - 2 \times C_s^n(i,j) + C_s^n(i,j-1)))}{dz^2} \right) - dt \times \left( \frac{k_1}{R_s} \times C_s^n(i,j) \right) \tag{17}$$

$$\frac{(C_s^n(i,1) - 2 \times C_s^n(i,0) + C_s^n(i,0))}{dz^2} \tag{18}$$

At time step  $n$ , the input sediment surface concentration  $C_s(i, 0)$  to the sediment equation is calculated from the water equation at the same time step because of the faster dispersion in the water phase compared to the diffusion in the sediment. At time step  $n+1$ , the input sediment surface concentration  $C_s(i,0)$  to the water equation is calculated from the sediment equation at time step  $n$ .

### 6 Analytical Equations

#### 6.1 Dynamic Solution to the Diffusion and Sedimentation Problem in the Sediment

A combined dynamic diffusion, sedimentation, and degradation problem is too complex to solve analytically. Determination of the concentration profile in the sediment at any given position in the fjord is therefore simplified to a problem of diffusion and sedimentation in a semi-infinite medium, where the boundary (water) is kept at a constant concentration. It is acceptable to consider the water concentration as constant in time due to the high horizontal dispersion and vertical mixing that prevail in the water phase compared to the slower sedimentation to and diffusion in the sediment. The boundary condition is thus  $C_s(x, 0) = C_w(x)_{\text{steady state}}$  for  $t > 0$ . The initial condition is  $C_s(x, z) = 0$  for  $t = 0$ . The solution of the one-dimensional diffusion and sedimentation problem, Eq. 19, thus yields Eq. 20 [13]. Where  $\text{erfc}(\ )$  is the complementary error function.

$$\frac{\partial C_s}{\partial t} = \frac{D_{sz}}{R_s} \times \frac{\partial^2 C_s}{\partial z^2} - S \times \frac{\partial C_s}{\partial z} \tag{19}$$

$$C_s = 0.5 \times C_w$$

$$\times \left( \text{erfc} \left( 0.5 \times \sqrt{\frac{R_s}{D_s}} \times \left( \frac{z}{\sqrt{t}} - S \times \sqrt{t} \right) \right) + e^{\frac{S \times R_s}{D_s}} \times \text{erfc} \left( 0.5 \times \sqrt{\frac{R_s}{D_s}} \times \left( \frac{z}{\sqrt{t}} + S \times \sqrt{t} \right) \right) \right) \tag{20}$$

#### 6.2 Steady-state Solution to the Diffusion, Sedimentation, and Degradation Problem in the Sediment

Under steady-state conditions, the linear homogeneous second-order equation, describing diffusion, sedimentation, and degradation in the sediment compartment, is as shown in Eq. 21. It can be solved according to Spiegel [14] with the boundary conditions  $C_s \rightarrow 0$  for  $z \rightarrow \infty$ ,  $C_s = C_w$  (steady state) for  $z = 0$ , giving Eq. 22.

$$\frac{D_{sz}}{R_s} \times \frac{d^2 C_s}{dz^2} - S \times \frac{dC_s}{dz} - \frac{k_1}{R_s} \times C_s = 0 \Leftrightarrow \frac{d^2 C_s}{dz^2} - \frac{S \times R_s}{D_{sz}} \times \frac{dC_s}{dz} - \frac{k_1}{D_{sz}} \times C_s = 0 \tag{21}$$

$$C_s(z) = C_w(\text{steady - state})$$

$$\times e^{\left( \frac{S \times R_s}{D_{sz} \times 2} \sqrt{\left( \frac{S \times R_s}{D_{sz} \times 2} \right)^2 + \frac{k_1}{D_{sz}}} \right) \times z} \tag{22}$$

### 7 Results and Discussion

#### 7.1 Theoretical Validation, Sediment Compartment

In Fig. 4, the numerical model, Eq. 17, is validated with the analytical solution to the diffusion and sedimentation

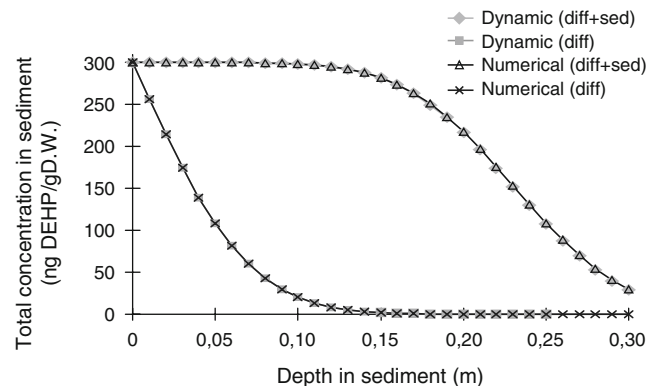


Fig. 4 Validation of numerical sediment model (Eq. 17) with analytical solution (Eq. 20)



problem, Eq. 20. Degradation is set to zero in the numerical model and the following parameters are used;  $S=2.5$  mm year<sup>-1</sup>,  $k_{1N}=2 \times 10^{-5}$  s<sup>-1</sup>,  $k_{1D}=8 \times 10^{-6}$  s<sup>-1</sup> (below a depth of 5 cm),  $K_d=10,000$  L water (kg dm)<sup>-1</sup>. Simulation time is 50 years and the optimum time step, with respect to run time and precision, is  $dt=10^5$  s. Vertical step size is  $dz=0.01$  m.

Two cases are considered: diffusion combined with sedimentation and diffusion alone. The sedimentation process in the numerical model, where discrete layers of thickness 1 cm are added, is seen to be satisfactorily described compared to the analytical solution. A situation of sedimentation alone will produce a horizontal curve through 300 ng DEHP g DM extending to a depth of  $S \times 50$  years  $\approx 12$  cm. The two diffusion curves and the two diffusion + sedimentation curves are coincident, which implies that the numerical sediment model is considered to be validated.

## 7.2 Experimental Calibration, Sediment Compartment

In Fig. 5, the validated numerical model is calibrated with the experimental sediment concentration profile sampled 130 m from the WWTP discharge. The curve at the upper 5 cm decreases according to the typical transport degradation situation with a constant degradation rate. The high degradation rate indicates aerobic conditions and is the same order of magnitude as the aerobic rate found in the WWTP although the biomass and oxygen concentrations are considerably lower in the sediment. Deeper down in the sediment, the profile flattens out and decreases with only 10% in 5 cm. The oxygen concentration is probably negligible. A degradation rate of  $8 \times 10^{-6}$  s<sup>-1</sup> suggests either anoxic or anaerobic conditions.

The periodic fluctuations from 12 to 20 cm are probably experimental noise but bioturbation by lugworm (*Arenicola*

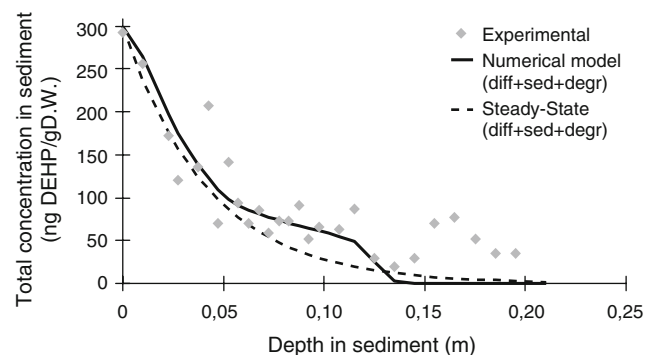


**Fig. 5** Experimental sediment core concentrations at distance 130 m from discharge, numerical sediment model (Eq. 17) and steady-state solution (Eq. 22)

*marina*) could also cause this effect. Circumstances that disconfirm this are the hardness of the sediment core. Two cases can be considered: the fluctuations below approximately 12 cm are noise and the concentrations are zero. This gives a sedimentation rate of 2.5 mm year<sup>-1</sup>. Alternatively, the concentration profile below 10 cm is approximately constant down to a depth of minimum 20 cm. In this case, the sedimentation is equal to or larger than 4.5 mm year<sup>-1</sup> since diffusion alone cannot transport this amount of substance down to these depths. In the model setup, the sedimentation is described as a discontinuous process where a layer of  $dz=1$  cm is added every 4 years but in reality the sedimentation occurs in two annual maxima, one in the spring and one in the autumn. The different sediment applications have been investigated in the numerical model and the results are identical.

In Fig. 5, the last curve is the steady-state profile, cf. Eq. 22. From observing the profile development in time and from flux considerations by Sørensen et al. [13], the time needed to achieve steady state is governed by the sediment accumulation rate. It is only for  $t=0$ , where the concentration gradient at the sediment surface is infinitely high, that diffusion will dominate the flux. With  $S=2.5$  mm year<sup>-1</sup>, steady state is reached in the upper 2.5 cm after 10 years.

Equation 23 shows the flux at the sediment surface during steady state. It is found by differentiating Eq. 22 for  $z=0$  and insertion in Eq. 13. Higher degradation rates yield increasing concentration gradients and thus higher diffusion rates through the sediment. Higher adsorption coefficients,  $K_d$ , and therefore higher retention factors,  $R_s$ , result in higher association with particulate matter and higher sedimentation rates of adsorbed substance. For DEHP, the ratio between  $k_{1N} \times D_{sz}=2.0 \times 10^{-15}$  m<sup>2</sup> s<sup>-2</sup> and  $S \times R_s=26.5$  m year<sup>-1</sup> gives in a sedimentation flux comprising about 95% of the total flux to the sediment. Hydrophobic substances are thus transported to the sediment at higher rates than hydrophilic substances.

$$N_{sz} = C_w(\text{steady} - \text{state}) \times S \times R_s \times \left( 0.5 + \sqrt{0.25 + \frac{k_1 \times D_{sz}}{(S \times R_s)^2}} \right) \quad (23)$$

## 7.3 Water Compartment

Experimental measurements in the water compartment yield a mean DEHP concentration of  $91 \pm 81$  ng DEHP per liter (five sampling sites) [20]. Water concentrations in the different sections of the fjord are calculated from Eq. 5, combining the two box models and the dispersion model in an iterate process. The calculations assume constant flows

and constant concentrations for the DEHP sources. Steady state will occur in the water compartment after a few months and will therefore be considered in the following. For simplicity reasons, the diffusive suction by the sediment is omitted, which is in accordance with steady state. The biomass concentration in the water is a factor of 100 lower than in the WWTP and furthermore the micro-organisms are not adapted to optimum DEHP degradation; therefore, the degradation rate per liter is set a factor of 1,000 lower than in the WWTP,  $k_1=2 \times 10^{-8} \text{ s}^{-1}$ . This is probably still too high but it is compensated by the removal by volatilization. Apart from the degradation rate, there are no adjustments of the model parameters in order to fit the modeled results to the experimental findings. The experimental sediment surface concentrations increase towards the inner parts of the fjord. In Roskilde Vig, the DEHP concentration is a factor of two higher than in the Bredning and a factor of ten higher than in the narrow passage. In the narrow passage, the flow and turbulence are considerably higher and the net sedimentation rate is reduced.

By using the calculated steady-state concentration for the Bredning as boundary condition in the numerical solution for the narrow passage, the water concentration profile in Fig. 6 is obtained. The experimental concentrations in the water compartment are approximately constant in all sections of the fjord and do therefore not display the characteristic decrease caused by dispersion as seen in Fig. 6. The experimental concentration peaks around 11 km (Frederiksund), which is an area with very high current and resuspension of settled material with adsorbed DEHP. With a mean experimental water concentration of 91 ng DEHP per liter, there is a discrepancy by a factor of 3–5 compared to the modeled water concentrations. A reason for the underestimation of the calculated concentrations could be missing contributions from sources such as boats, spills from industrial activities, or leaching from dumped slag which is reported to have taken place in the Vig.

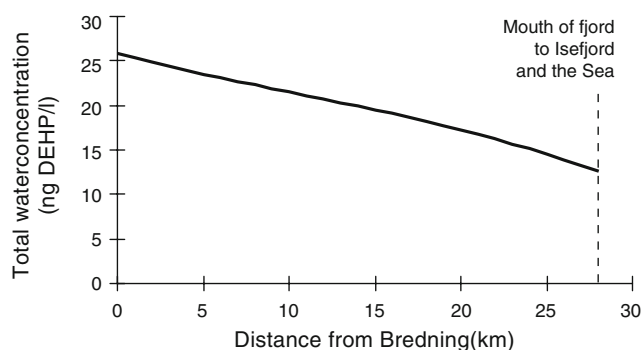


**Fig. 6** Total DEHP concentrations in water in the narrow passage, numerical model (Eq. 15)

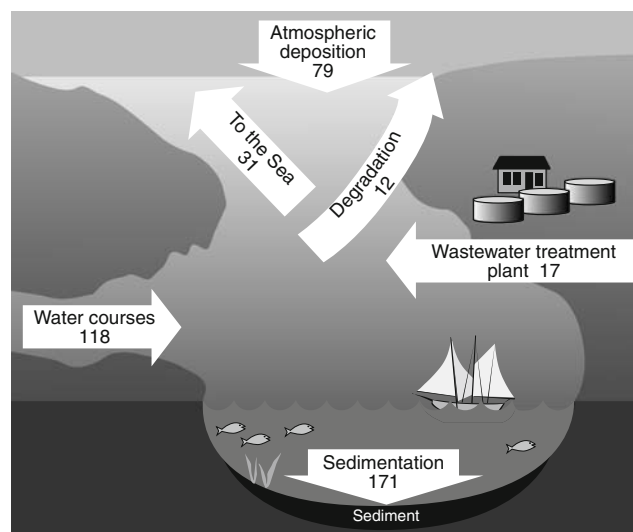


**Fig. 7** Flow of DEHP in gram per day for the entire Roskilde fjord, calculated from the water and sediment models

#### 7.4 Flow of DEHP in and Around Roskilde Fjord

In Fig. 7, the DEHP sources, removals, and sinks to the Roskilde fjord water compartment are shown as steady-state mean flows ( $\text{g DEHP day}^{-1}$ ). The freshwater sources from streams are the main contributors to DEHP in the fjord water followed by atmospheric deposition and WWTP discharges. The removal processes are highly dominated by sedimentation, followed by water exchange with the sea and degradation balancing the sources. Calculated steady-state mean water concentrations for the three regions of the fjord are Vig 32 ng DEHP per liter, Bredning 26 ng DEHP per liter, and narrow passage 19 ng DEHP per liter (mean, cf. Fig. 6).

## 8 Conclusions

The cycle of the phthalate ester DEHP is investigated in a typical Danish rural environment, where the main sources, removal processes, and sinks are quantified in the recipient Roskilde fjord. Sedimentation of particle-bound DEHP, or binding of dissolved DEHP to sediments, is the main removal process from the water compartment, whereas degradation and transport to the surrounding sea are of lesser significance. Freshwater from streams is the main source and is followed by atmospheric deposition and discharges from wastewater treatment plants.

Numerical models are set up to quantify the transport of DEHP in the water and sediment compartments of the fjord and a steady-state mass balance quantifies the DEHP flow in and around Roskilde fjord. Calculated DEHP concentrations in the water are validated with measured fjord water

concentrations and the sediment model is calibrated with sediment core measurements and validated with analytical solutions.

The fate of DEHP in the sediment compartment is described with sedimentation, diffusion, and first-order degradation. However, diffusion can be omitted under steady-state conditions, which typically occur in the surface layer after about 10 years. The insignificance of gradient conditioned diffusion in the surface layer justifies the use of a sediment description comprising a totally mixed sediment compartment, such as the setup used in the mathematically simpler SimpleBox, comprised in the European Union System for the Evaluation of Substances. The suggested modeling approach, where water and sediment compartments are treated separately only connected with substance exchange through sedimentation, seems appropriate in describing the fate of DEHP in Roskilde fjord.

The model requires a set of predefined processes and parameters that are valid for the specific conditions represented by Roskilde fjord. These conditions are highly influential on the model result. For other fjords and inner waters, the conditions will be different and by adjusting the parameters the model setup may still be applicable. It is important to always have some means of validation of model calculations, either with other models or most appropriately measurements in the actual system.

Concentrations found in the fjord water are too low to adversely affect the environment, whereas the concentrations found in the sediments may influence the bottom living organism and through them enter the food chain. The suggested net DEHP supply to the sediment may further build up the DEHP concentration and eventually cause critical levels in the water phase in the future. The presented fate model elucidates the transport patterns of DEHP in the complex multimedia fjord system and can support decision making as to which sources must be reduced in order to implement the most effective strategy for protecting man and the environment.

## References

- European Chemicals Bureau (ECB) (2001). RISK ASSESSMENT bis(2-ethylhexyl) phthalate, CAS-No.: 117-81-7, EINECS-No.: 204-211-0. <http://ecb.jrc.it/esis/index.php?PGM=hpv>. Accessed Jan 2008.
- Fauser, P., Sørensen, P. B., Vikelsøe, J., & Carlsen, L. (2000). Phthalates, nonylphenols and LAS in Roskilde wastewater treatment plant—fate modelling based on measured concentrations in wastewater and sludge. Ministry of Environment and Energy, National Environmental Research Institute, Department of Environmental Chemistry, Research Report 354.
- Fauser, P., Vikelsøe, J., Sørensen, P. B., & Carlsen, L. (2003). Phthalates, nonylphenols and LAS in an alternately operated wastewater treatment plant – fate modelling based on measured concentrations in wastewater and sludge. *Water Research*, 37, 1288–1295. doi:10.1016/S0043-1354(02)00482-7.
- Furtmann, K. (1996). Phthalates in the aquatic environment. Landesamt für Wasser und Abfall Nordrhein-Westfalen.
- Gerritsen, J., Holland, A. F., & Irvine, D. E. (1994). Suspension feeding bivalves and the fate of primary production: An estuarine model applied to Chesapeake Bay. *Estuaries*, 17, 403–416. doi:10.2307/1352673.
- Harremoës, P., & Malmgren-Hansen, A. (Red.) (1990). Lærebog i Vandforurening (in Danish). Polyteknisk Forlag, ISBN 87-502-0671-0.
- Hedal, S., Hansen, L. R., Thingberg, C., & Jensen, K. B. (1999). Overvågning af Roskilde fjord 1998. Roskilde Amt, Teknisk Forvaltning og Frederiksborg Amt, Teknik og Miljø.
- Kao, P. H., Lee, F. Y., & Hseu, Z. Y. (2005). Sorption and biodegradation of phthalic acid esters in freshwater sediments. *Journal of Environmental Science and Health. Part A, Toxic/Hazardous Substances & Environmental Engineering*, 40, 103–115. doi:10.1081/ESE-200033605.
- Kroschwitz, J. I. (1998). *Kirk-Othmer encyclopedia of chemical technology* (4th ed.). New York: Wiley.
- Madsen, P. P., & Larsen, B. (1979). Bestemmelse af Akkumulationsrater i Marine Sedimentationsområder ved Pb-210 Datering. *Vand*, 5, 2–6 in Danish.
- Rasmussen, B., & Josefson, A. B. (2002). Consistent estimates for the residence time of micro-tidal estuaries. *Estuarine, Coastal and Shelf Science*, 64, 65–73.
- Schwarzenbach, R., Gschwend, P. M., & Imboden, D. (2003). *Environmental organic chemistry* (2nd ed.). Hoboken: Wiley.
- Sørensen, P. B., Fauser, P., Carlsen, L., & Vikelsøe, J. (2000). Evaluation of sub-process validity in the TGD in relation to hydrophobic substances. Ministry of Environment and Energy, National Environmental Research Institute, Department of Environmental Chemistry, Research Report.
- Spiegel, M. R. (1968). *Mathematical handbook of formulas and tables. Schaum's outline series*. New York: McGraw-Hill.
- Stigebrandt, A. (2001). Fjordenv—a water quality model for fjords and other inshore waters. Department of Oceanography, Göteborg University, ISSN 1400-383X.
- Skårup, S. & Skytte, L. (COWI A/S) (2003). Forbruget af PVC og phthalater i Danmark år 2000 og 2001. Kortlægning af Kemiske Stoffer i Forbrugerprodukter nr. 35 2003.
- Thomsen, M., & Carlsen, L. (1998). Phthalater I Miljøet: Opløselighed, Sorption Og Transport (in Danish). Danish National Environmental Research Institute. Research Report No. 249, pp 120.
- Thomsen, M., Carlsen, L., & Hvidt, S. (2001). Solubilities and surface activities of phthalates investigated by surface tension measurements. *Environmental Toxicology and Chemistry*, 20, 127–132. doi:10.1897/1551-5028(2001)020<0127:SASAOP>2.0.CO;2.
- Turner, A., & Rawling, M. C. (2000). The behaviour of di-(2-ethylhexyl) phthalate in estuaries. *Marine Chemistry*, 68, 203–217. doi:10.1016/S0304-4203(99)00078-X.
- Vikelsøe, J., Fauser, P., Sørensen, P. B., Carlsen, L. (2001). Phthalates and nonylphenols in Roskilde fjord—a field study and mathematical modelling of transport and fate in water and sediment. Ministry of Environment and Energy, National Environmental Research Institute, Department of Environmental Chemistry, Technical Report No 339.
- Vikelsøe, J., Thomsen, M., Johansen, E., & Carlsen, L. (1999). Phthalates and nonylphenols in soil—a field study of different soil profiles. Ministry of Environment and Energy, National Environmental Research Institute, Department of Environmental Chemistry, Technical Report No. 268.

22. Wiggers, L., Nykrog, J., & Juhler, L. (2000). Nutrients in and discharges from Streams in Aarhus County, 1999 (in Danish). Århus Amt, Natur- og Miljøkontoret, Teknisk Rapport, ISBN 87-7906-108-7.
23. Williams, M. D., Adams, W. J., & Parkerton, T. F. (1995). Sediment sorption coefficient measurements for 4 phthalate-esters - experimental results and model-theory. *Environmental Toxicology and Chemistry*, 14, 1477–1486. doi:10.1897/1552-8618(1995)14[1477:SSCMFF]2.0.CO;2.
24. Zhou, J. L., & Liu, Y. P. (2000). Kinetics and equilibria of the interactions between diethylhexyl phthalate and sediment particles in simulated estuarine systems. *Marine Chemistry*, 71, 165–176. doi:10.1016/S0304-4203(00)00047-5.